

DOI: <https://doi.org/10.15407/pmach2024.02.025>

UDC 539.3

ANALYSIS OF THE STRESS STATE OF A LAYER WITH TWO CYLINDRICAL SWIVEL JOINTS AND A CYLINDRICAL CAVITY

Vitalii Yu. Miroshnikovv.miroshnikov@khai.edu

ORCID: 0000-0002-9491-0181

Valentyn P. Pelykhvenator.verba@gmail.com

ORCID: 0009-0007-5301-6697

Oleksandr Yu. DenshchykovAlex_day@ukr.net

ORCID: 0009-0008-2385-5841

National Aerospace University
"Kharkiv Aviation Institute"17, Vadyma Manka str., Kharkiv,
61070, Ukraine

In practice, connections in the form of cylindrical swivel joints are often encountered. However, exact methods for calculating such models are absent. Therefore, the development of algorithms to solve such problems is relevant. In this study, a spatial elasticity problem is solved for an infinite layer with two cylindrical swivel joints and a cylindrical cavity positioned parallel to each other and parallel to the layer surfaces. The embedded cylindrical swivel joints are represented as cavity with given contact-type conditions (normal displacements and tangential stresses). Stresses are specified on the layer surfaces and the cavity surface. The layer is considered in a Cartesian coordinate system, while the cylindrical cavities are considered in local cylindrical coordinates. The spatial elasticity problem is solved using the generalized Fourier method applied to the Lamé equations. Satisfying the boundary conditions results in a system of infinite linear algebraic equations, which undergo reduction methods. In the numerical study, the accuracy of boundary condition fulfillment reached 10^{-3} for stress values ranging from 0 to 1, with the equation system (Fourier series members) order of $m=4$. As the order of the system equations increases, the accuracy of calculations increases. Stress state analysis was conducted at varying distances between supports. The obtained results indicate that with an increased distance between supports, stresses on the supporting cylindrical surfaces of the layer and the cylindrical cavity surface decrease. These stresses are redistributed to the upper and lower surfaces of the layer, where the stresses increase and exceed the specified ones. The numerical outcomes can be applied to predict geometric parameters during design processes.

Keywords: layer with cylindrical cavities, generalized Fourier method, contact-type conditions.

Introduction

When designing parts of machines and mechanisms in the fields of machine and aircraft construction, it is necessary to have the most accurate distribution of the stress state in the body. For this reason, it is important to choose the most accurate method of the calculation results obtaining.

During such design, models with a connection in the form of a cylindrical swivel joints are often found.

Currently, similar problems are solved by methods of construction mechanics or numerical methods, such as the finite element method [1, 2]. Thus, the study [3] uses the finite element method to analyze the stress-strain state of a half-space supported by a plate with a vertical cylindrical cavity and a reinforced shell.

This work is licensed under a Creative Commons Attribution 4.0 International License.

© Vitalii Yu. Miroshnikov, Valentyn P. Pelykh, Oleksandr Yu. Denshchykov, 2024

However, the assumptions of construction mechanics methods allow a significant change in the model, and numerical methods are approximate and do not take into account the infinite boundaries of the body. This does not give high accuracy and confidence in the final result [4].

The use of analytical methods [5, 6] gives accurate results, but they cannot take into account more than three spatial boundary surfaces.

Many papers are devoted to a layer with a cylindrical cavity or an inclusion perpendicular to their surface [7–11]. One of the approaches to solving this problem consists in solving the problem for a layer with a cylindrical cavity assuming ideal contact conditions at the upper and lower boundaries of the layer [7]. A similar situation was also considered in [8], when the lower surface of the layer was rigidly fixed. These studies [7, 8] used integral Laplace transforms and integral sine and cosine Fourier transforms. These methods are applied to boundary conditions and axisymmetric equations of motion, which create a one-dimensional vector inhomogeneous boundary value problem. However, they cannot help effectively solve problems with multiple boundary surfaces and are limited to solving only wave diffraction problems.

In the study [9], stress analysis of perforated plates was carried out using genetic algorithm (GA), gravity search algorithm (GSA) and Bat algorithm (BA). However, the used methods are also approximate and do not guarantee the accuracy of the final result.

The torsion of an elastic half-space with a vertical cylindrical cavity and a coax was considered in the paper [10]. The problem was reduced to integral equations of the second kind, which made it possible to obtain highly accurate values of the stress state of the body.

In the study [11], for composite laminated plates with circular cross-sections, an analytical solution based on the method of layer whipping was developed. However, the methods used in these problems with the transverse arrangement of the cavity or inclusion [5, 6] cannot be used to solve the problem for a layer with longitudinal cylindrical cavities.

The specified type of problems can also be solved by the methods used for the calculation of composite materials. These methods make it possible to take into account the nonlinearity of the given model. At the same time, cylindrical swivel joints supports can be considered as completely rigid elements. Similar methods are used in papers [12–15]. Thus, in [12], the problem of determining the dynamic stress state in two overlapped rods of different lengths is considered. The load is modeled by a longitudinal force applied to one of the rods. The Holland-Reissner adhesive joint model was used during the solution. The paper [13] studied the behavior of multilayer structures during the action of a dynamic load on them during a transverse impact. The theory of two-dimensional discrete structure is used for the solution. At the same time, the solution is based on the decomposition of the displacement vector of each layer into a power series. Theoretically obtained results correlate with experimental data obtained during research. Papers [14] and [15] are devoted to the study of the stress state in aviation multilayer glass units. At the same time, in [14], the glass unit is considered as an open cylindrical multilayer shell of constant thickness, and the thermal stress state arises from the action of interlayer film heat sources. An analytical solution was obtained for the described problem. The paper [15] is devoted to the creation of a method for assessing the strength of a multilayer glass unit in case of a collision with a bird and a method for assessing excess pressure in the case of a specified collision. For the solution, a refined theory of taking into account the first order of transverse shear deformations, reducing the thickness and rotation inertia of the element of each layer is used.

A general drawback of the methods used in papers [12–15] is the impossibility of taking into account zero displacements in the contact zones with cylindrical joints.

To take into account the longitudinal inhomogeneities in the layer, the analytical-numerical generalized Fourier method [16] is the most effective. This method allows to use the transition functions between the basic solutions of the Lamé equation to combine the solutions of the problem in different coordinate systems.

Thus, with the help of the generalized Fourier method, problems for an elastic cylinder with cylindrical cavities [17, 18] or cylindrical inclusions [19], as well as for a half-space with a spheroidal cavity [20] were solved. However, to calculate a layer with a cylindrical cavity, it is necessary to use the formulas for the transition of basic solutions between cylindrical and Cartesian coordinate systems.

Such transition formulas are considered for a half-space with a cylindrical cavity in paper [21], for a layer with a cylindrical cavity in papers [22, 23], for a layer with a continuous cylindrical inclusion in paper [24] and a layer with a cylindrical thick-walled pipe in paper [25]. However, these papers [21–25] do not apply the

formulas of the transition between local cylindrical coordinate systems, which does not allow to solve the problem with several cylindrical inhomogeneities.

In paper [26], the problem was solved for a layer with two cylindrical supports embedded into it, and in paper [27], the problem was solved for a layer with two continuous cylindrical inclusions and mixed boundary conditions. However, in these papers, the transition formulas between shifted cylinders are not used, which allows to consider only two cylindrical inhomogeneities.

In paper [28], the problem of the theory of elasticity for a rigidly connected layer with three embedded supports is solved. It also takes into account the transition formulas between displaced cylinders, but a different type of boundary conditions (displacement) is applied to the surfaces of the cavities. However, for the calculation of a problem containing a cylindrical swivel joint, it is necessary to apply the conditions of the contact type.

Considering the availability of calculation schemes in the form of a layer with cylindrical swivel joints and a cylindrical cavity, the creation of a method for calculating such problems is relevant. Therefore, the generalized Fourier method will be used for high-precision calculation.

Problem statement

The elastic homogeneous layer is located on two cylindrical swivel joints embedded into it and has a longitudinal cylindrical cavity that is parallel to its borders (Fig. 1).

Embedded cylindrical swivel joints will be presented as cavities with contact type conditions set for them. We denote the radii of the cavities as R_p , where p – cavity number. The layer is given in the Cartesian coordinate system (x, y, z) , cavities are given in local cylindrical coordinate systems (ρ_p, φ_p, z) . Distance to layer boundaries is $y=h$ and $y=-\tilde{h}$.

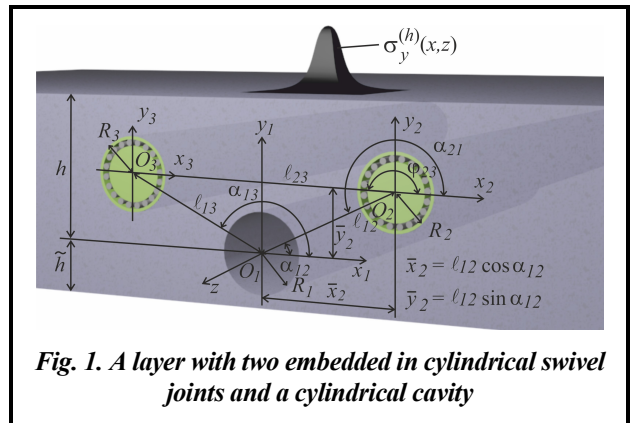


Fig. 1. A layer with two embedded in cylindrical swivel joints and a cylindrical cavity

It is necessary to find a solution to the Lamé equation $\Delta \bar{u} + (1 - 2\sigma)^{-1} \nabla \text{div} \bar{u} = 0$.

Stresses are set on the upper and lower boundaries of the layer, as well as on the surface of the first cavity $F\bar{U}(x, z)|_{y=h} = \bar{F}_h^0(x, z)$, $F\bar{U}(x, z)|_{y=-\tilde{h}} = \bar{F}_{\tilde{h}}^0(x, z)$, $F\bar{U}(\varphi_1, z)|_{\rho_1=R_1} = \bar{U}_0^{(1)}(\varphi_1, z)$ respectively, where \bar{U} – displacement in a layer;

$$\begin{aligned} \bar{F}_h^0(x, z) &= \tau_{yx}^{(h)} \bar{e}_x + \sigma_y^{(h)} \bar{e}_y + \tau_{yz}^{(h)} \bar{e}_z, \\ \bar{F}_{\tilde{h}}^0(x, z) &= \tau_{yx}^{(\tilde{h})} \bar{e}_x + \sigma_y^{(\tilde{h})} \bar{e}_y + \tau_{yz}^{(\tilde{h})} \bar{e}_z, \quad \text{– known functions.} \\ \bar{U}_0^{(1)}(\varphi_1, z) &= \sigma_\rho^{(1)} \bar{e}_\rho + \tau_{\rho\varphi}^{(1)} \bar{e}_\varphi + \tau_{\rho z}^{(1)} \bar{e}_z \end{aligned} \tag{1}$$

On the surfaces of cavities $p=2, p=3$ normal displacements and tangential stresses are given.

$$\left. \begin{aligned} U_\rho(\varphi_p, z)|_{\rho_p=R_p} &= U_0^{(p)}(\varphi_p, z), \\ \tau_{\rho\varphi}|_{\rho_p=R_p} &= \tau_1^{(p)}(\varphi_p, z), \\ \tau_{\rho z}|_{\rho_p=R_p} &= \tau_2^{(p)}(\varphi_p, z) \end{aligned} \right\} \tag{2}$$

We consider all given functions to be rapidly decreasing from the origin of the coordinates along the axis z and axis x .

Solution method

We choose the basic solutions of the Lamé equation for Cartesian and cylindrical coordinate systems in the form [16]

$$\begin{aligned} \bar{u}_k^\pm(x, y, z; \lambda, \mu) &= N_k^{(d)} e^{i(\lambda z + \mu x) \pm i \gamma y}, \\ \bar{R}_{k,m}(\rho, \varphi, z; \lambda) &= N_k^{(p)} I_m(\lambda \rho) e^{i(\lambda z + m \varphi)}, \\ \bar{S}_{k,m}(\rho, \varphi, z; \lambda) &= N_k^{(p)} \left[(\text{sign } \lambda)^m K_m(|\lambda| \rho) \cdot e^{i(\lambda z + m \varphi)} \right]; \quad k = 1, 2, 3; \end{aligned} \tag{3}$$

$$N_1^{(d)} = \frac{1}{\lambda} \nabla; N_2^{(d)} = \frac{4}{\lambda} (\sigma - 1) \bar{e}_2^{(1)} + \frac{1}{\lambda} \nabla(y \cdot); N_3^{(d)} = \frac{i}{\lambda} \text{rot}(\bar{e}_3^{(1)} \cdot); N_1^{(p)} = \frac{1}{\lambda} \nabla;$$

$$N_2^{(p)} = \frac{1}{\lambda} \left[\nabla \left(\rho \frac{\partial}{\partial \rho} \right) + 4(\sigma - 1) \left(\nabla - \bar{e}_3^{(2)} \frac{\partial}{\partial z} \right) \right]; N_3^{(p)} = \frac{i}{\lambda} \text{rot}(\bar{e}_3^{(2)} \cdot); \gamma = \sqrt{\lambda^2 + \mu^2}, \quad -\infty < \lambda, \mu < \infty,$$

where $I_m(x), K_m(x)$ are modified Bessel functions; $\bar{R}_{k,m}, \bar{S}_{k,m}$ are inner and outer solutions of the Lamé equation for the cylinder, respectively; $\bar{u}_k^{(-)}, \bar{u}_k^{(+)}$ are solutions of the Lamé equation for a layer; σ is the Poisson's ratio.

We will present the solution of the problem in the form [28]

$$\bar{U} = \sum_{p=1}^3 \sum_{k=1}^3 \int_{-\infty}^{\infty} \sum_{m=-\infty}^{\infty} B_{k,m}^{(p)}(\lambda) \cdot \bar{S}_{k,m}(\rho_p, \varphi_p, z; \lambda) d\lambda +$$

$$+ \sum_{k=1}^3 \int_{-\infty}^{\infty} \int_{-\infty}^{\infty} (H_k(\lambda, \mu) \cdot \bar{u}_k^{(+)}(x, y, z; \lambda, \mu) + \tilde{H}_k(\lambda, \mu) \cdot \bar{u}_k^{(-)}(x, y, z; \lambda, \mu)) d\mu d\lambda \quad (4)$$

where $\bar{S}_{k,m}(\rho_p, \varphi_p, z; \lambda), \bar{u}_k^{(+)}(x, y, z; \lambda, \mu)$ i $\bar{u}_k^{(-)}(x, y, z; \lambda, \mu)$ are basic solutions given by formulas (3), and unknown functions $H_k(\lambda, \mu), \tilde{H}_k(\lambda, \mu), B_{k,m}^{(p)}(\lambda)$ must be found from boundary conditions (1) and (2).

The transition between basic solutions in different coordinate systems will be carried out using formulas [16]:

– for the transition from basic solutions $\bar{S}_{k,m}$ of the cylindrical coordinate system to layer solutions $\bar{u}_k^{(-)}$ (at $y > 0$) and $\bar{u}_k^{(+)}$ (at $y < 0$)

$$\bar{S}_{k,m}(\rho_p, \varphi_p, z; \lambda) = \frac{(-i)^m}{2} \int_{-\infty}^{\infty} \omega_{\mp}^m \cdot e^{-i\mu \bar{x}_p \pm \gamma \bar{y}_p} \cdot \bar{u}_k^{(\mp)} \cdot \frac{d\mu}{\gamma}, \quad k = 1, 3;$$

$$\bar{S}_{2,m}(\rho_p, \varphi_p, z; \lambda) = \frac{(-i)^m}{2} \int_{-\infty}^{\infty} \omega_{\mp}^m \cdot \left(\left(\pm m \cdot \mu - \frac{\lambda^2}{\gamma} \pm \lambda^2 \bar{y}_p \right) \bar{u}_1^{(\mp)} \mp \lambda^2 \bar{u}_2^{(\mp)} \pm 4\mu(1 - \sigma) \bar{u}_3^{(\mp)} \right) \cdot \frac{e^{-i\mu \bar{x}_p \pm \gamma \bar{y}_p} d\mu}{\gamma^2}, \quad (5)$$

where $\gamma = \sqrt{\lambda^2 + \mu^2}, \omega_{\mp}(\lambda, \mu) = \frac{\mu \mp \gamma}{\lambda}, m = 0, \pm 1, \pm 2, \dots;$

– for the transition from basic solutions $\bar{u}_k^{(+)}$ and $\bar{u}_k^{(-)}$ of the layer to solutions $\bar{R}_{k,m}$ of the cylindrical coordinate system

$$\bar{u}_k^{(\pm)}(x, y, z) = e^{i\mu \bar{x}_p \pm \gamma \bar{y}_p} \cdot \sum_{m=-\infty}^{\infty} (i \cdot \omega_{\mp})^m \bar{R}_{k,m}, \quad (k = 1, 3);$$

$$\bar{u}_2^{(\pm)}(x, y, z) = e^{i\mu \bar{x}_p \pm \gamma \bar{y}_p} \cdot \sum_{m=-\infty}^{\infty} \left[(i \cdot \omega_{\mp})^m \cdot \lambda^{-2} \left((m \cdot \mu + \bar{y}_p \cdot \lambda^2) \cdot \bar{R}_{1,m} \pm \gamma \cdot \bar{R}_{2,m} + 4\mu(1 - \sigma) \bar{R}_{3,m} \right) \right], \quad (6)$$

where $\bar{R}_{k,m} = \tilde{b}_{k,m}(\rho_p, \lambda) \cdot e^{i(m\varphi_p + \lambda z)}; \tilde{b}_{1,n}(\rho, \lambda) = \bar{e}_\rho \cdot I'_n(\lambda \rho) + i \cdot I_n(\lambda \rho) \cdot \left(\bar{e}_\varphi \frac{n}{\lambda \rho} + \bar{e}_z \right);$

$$\tilde{b}_{2,n}(\rho, \lambda) = \bar{e}_\rho \cdot [(4\sigma - 3) \cdot I'_n(\lambda \rho) + \lambda \rho I''_n(\lambda \rho)] + \bar{e}_\varphi \cdot i \cdot m \left(I'_n(\lambda \rho) + \frac{4(\sigma - 1)}{\lambda \rho} I_n(\lambda \rho) \right) + \bar{e}_z \cdot i \lambda \rho I'_n(\lambda \rho);$$

$\tilde{b}_{3,n}(\rho, \lambda) = \left[\bar{e}_\rho \cdot I_n(\lambda \rho) \frac{n}{\lambda \rho} + \bar{e}_\varphi \cdot i \cdot I'_n(\lambda \rho) \right]; \bar{e}_\rho, \bar{e}_\varphi, \bar{e}_z$ are coordinates in the cylindrical coordinate system;

– for the transition from the basic solutions of the cylinder with the number p to the solutions of the cylinder with the number q

$$\begin{aligned} \bar{S}_{k,m}(\rho_p, \varphi_p, z; \lambda) &= \sum_{n=-\infty}^{\infty} \bar{b}_{k,pq}^{mn}(\rho_q) \cdot e^{i(n\varphi_q + \lambda z)}, k=1, 2, 3; \\ \bar{b}_{1,pq}^{mn}(\rho_q) &= (-1)^n \tilde{K}_{m-n}(\lambda \ell_{pq}) \cdot e^{i(m-n)\alpha_{pq}} \cdot \tilde{b}_{1,n}(\rho_q, \lambda); \\ \bar{b}_{3,pq}^{mn}(\rho_q) &= (-1)^n \tilde{K}_{m-n}(\lambda \ell_{pq}) \cdot e^{i(m-n)\alpha_{pq}} \cdot \tilde{b}_{3,n}(\rho_q, \lambda); \end{aligned} \quad (7)$$

$$\bar{b}_{2,pq}^{mn}(\rho_q) = (-1)^n \left\{ \tilde{K}_{m-n}(\lambda \ell_{pq}) \cdot \tilde{b}_{2,n}(\rho_q, \lambda) - \frac{\lambda}{2} \ell_{pq} \cdot [\tilde{K}_{m-n+1}(\lambda \ell_{pq}) + \tilde{K}_{m-n-1}(\lambda \ell_{pq})] \cdot \tilde{b}_{1,n}(\rho_q, \lambda) \right\} \cdot e^{i(m-n)\alpha_{pq}},$$

where α_{pq} is the angle between the axis x_p and segment ℓ_{pq} , $\tilde{K}_m(x) = (\text{sign}(x))^m \cdot K_m(|x|)$.

The distance and angle of rotation between parallel shifted cavities is calculated by formulas

$$\begin{aligned} L_{pq} &= \begin{cases} \sqrt{L_{1p}^2 + L_{1q}^2 - 2 \cdot L_{1p} \cdot L_{1q} \cdot \cos(\alpha_{1q} - \alpha_{1p})}, & \text{at } \alpha_{1q} \geq \alpha_{1p} \\ \sqrt{L_{1p}^2 + L_{1q}^2 - 2 \cdot L_{1p} \cdot L_{1q} \cdot \cos(\alpha_{1p} - \alpha_{1q})}, & \text{at } \alpha_{1q} < \alpha_{1p} \end{cases}; \\ \alpha_{pq} &= \begin{cases} \alpha_{1p} - \arccos\left(\frac{L_{1p}^2 + L_{pq}^2 - L_{1q}^2}{2 \cdot L_{1p} \cdot L_{pq}}\right) + \pi, & \text{at } \alpha_{1q} \geq \alpha_{1p} \\ \alpha_{1p} - \arccos\left(\frac{L_{1p}^2 + L_{pq}^2 - L_{1q}^2}{2 \cdot L_{1p} \cdot L_{pq}}\right) - \pi, & \text{at } \alpha_{1q} < \alpha_{1p} \end{cases}. \end{aligned}$$

To take into account the boundary conditions on the upper and lower boundaries of the layer, we apply the transition formulas (5) to the function (4), rewriting the basic solutions $\bar{S}_{k,m}(\rho_p, \varphi_p, z; \lambda)$ in the Cartesian coordinate system through $\bar{u}_k^{(-)}(x, y, z; \lambda, \mu)$ at $y=h$ and $\bar{u}_k^{(+)}(x, y, z; \lambda, \mu)$ at $y=-\tilde{h}$. After that, we will apply the stress operator to the right part. We equate the obtained vector with $y=h$ to the given $\bar{F}_h^0(x, z)$, and $y=-\tilde{h}$ to the given $\bar{F}_{\tilde{h}}^0(x, z)$, which we will first present through the double Fourier integral. After getting rid of the integrals in the right and left parts, we get six equations (one for each projection) with 15 unknowns $H_k(\lambda, \mu)$, $\tilde{H}_k(\lambda, \mu)$, $B_{k,m}^{(p)}(\lambda)$.

From this system of equations, we find $H_k(\lambda, \mu)$ and $\tilde{H}_k(\lambda, \mu)$ through $B_{k,m}^{(p)}(\lambda)$.

To take into account the boundary conditions in the stresses on the cavity $p=1$, we rewrite the basic solutions of the second $\bar{S}_{k,m}(\rho_2, \varphi_2, z; \lambda)$ and the third $\bar{S}_{k,m}(\rho_3, \varphi_3, z; \lambda)$ cylinders through basic solutions $\bar{R}_{k,m}(\rho_1, \varphi_1, z; \lambda)$ of the first cylinder, applying the transition formulas (7). We will also rewrite the basic solutions $\bar{u}_k^{(-)}(x, y, z; \lambda, \mu)$ and $\bar{u}_k^{(+)}(x, y, z; \lambda, \mu)$ of the layer through basic solutions $\bar{R}_{k,m}(\rho_1, \varphi_1, z; \lambda)$ of the first cylinder, applying the transition formulas (6). After that, we apply the stress operator to this right-hand side. The resulting vector at $\rho_1=R_1$, will be equal to the given one $\bar{U}_0^{(1)}(\varphi_1, z)$, which is represented by the Fourier series and integral. So, we get three equations for the first cylinder.

To take into account the boundary conditions of the contact type on the cavities $p=2, p=3$, we rewrite the right-hand part of (4) using the transition formulas (5) and (6) in the local cylindrical coordinate system of each cavity $p \neq 1$ through basic solutions $\bar{R}_{k,m}, \bar{S}_{k,m}$. After that, we will rewrite these basic solutions for $k=2$ and $k=3$ in terms of stresses. The resulting vector, at $\rho_p=R_p$, will be equated to the given one (2), represented by the Fourier series and integral. So, we get six equations for the second and third cylinders.

As a result, for each cylinder with the number p , we get three infinite systems of linear algebraic equations with respect to $B_{k,m}^{(p)}(\lambda)$, which contain $H_k(\lambda, \mu)$ and $\tilde{H}_k(\lambda, \mu)$. Thus, we will get 9 integral-algebraic

equations from $H_k(\lambda, \mu)$, $\tilde{H}_k(\lambda, \mu)$, $B_{k,m}^{(p)}(\lambda)$. Excluding the previously found $H_k(\lambda, \mu)$ and $\tilde{H}_k(\lambda, \mu)$ from these equations through $B_{k,m}^{(p)}(\lambda)$ and getting rid of the series over m and integrals over λ , we will get 9 infinite linear algebraic equations of the second kind to determine the unknowns $B_{k,m}^{(p)}(\lambda)$.

Found unknowns $B_{k,m}^{(p)}(\lambda)$ will be substituted in the expression for $H_k(\lambda, \mu)$ and $\tilde{H}_k(\lambda, \mu)$. In this way, all the unknowns of expression (4) will be found.

The reduction method is applied to the obtained infinite systems of equations. The accuracy of the fulfillment of the boundary conditions during the numerical study showed a high convergence of the solution of this system of linear algebraic equations.

Numerical studies of the stress state

The elastic isotropic layer contains two cylindrical joints and a cylindrical cavity (Fig. 1). Physical characteristics of the material (ABS plastic): Poisson's ratio $\sigma=0.38$, modulus of elasticity $E=1700 \text{ N/mm}^2$. Geometric parameters of the model: $R_1=R_2=R_3=5 \text{ mm}$, $h=15 \text{ mm}$, $\tilde{h}=15 \text{ mm}$, $\alpha_{12}=0$, $\alpha_{13}=\pi$. The distance between the cavities is chosen in two options $L_{12}=L_{13}=30 \text{ mm}$ and $L_{12}=L_{13}=40 \text{ mm}$.

Normal stresses in the form of a unit wave are set at the upper boundary of the layer $\sigma_y^{(h)}(x, z) = -10^8 \cdot (z^2 + 10^2)^{-2} \cdot (x^2 + 10^2)^{-2}$ and zero tangential stresses $\tau_{yx}^{(h)} = \tau_{yz}^{(h)} = 0$, at the lower boundary of the layer – zero stresses $\sigma_y^{(\tilde{h})}(x, z) = \tau_{yx}^{(\tilde{h})}(x, z) = \tau_{yz}^{(\tilde{h})}(x, z) = 0$. Zero stresses are set on the cavity $p=1$ $\sigma_p^{(i)} = \tau_{\rho\phi}^{(i)} = \tau_{\rho z}^{(i)} = 0$, contact type conditions are given $U_0^{(p)}(\phi, z) = \tau_1^{(p)}(\phi, z) = \tau_2^{(p)}(\phi, z) = 0$ on cavities $p=2, p=3$.

The infinite system was truncated by the parameter $m=4$ (the number of members of the Fourier series and the order of the system of equations).

The accuracy of the fulfillment of the boundary conditions for the specified m and the specified geometric parameters is not less than 10^{-3} with values from 0 to 1. This corresponds to the paper [22], where a thorough analysis of the convergence of the results at different values of m and the distance between the layer and the cavities was carried out.

Fig. 2 shows a graph of specified stresses σ_y and their corresponding stresses σ_x on the upper and lower surfaces of the layer at $z=0$.

The stress state (Fig. 2) indicates that the upper part of the layer is compressed, the lower part is stretched. This is physically correct compared to a beam on two supports.

When increasing the distance between supports, stresses σ_x on the upper and lower surfaces of the layer increase and exceed the specified values. The maximum stress values occur on the upper surface of the layer and at $L_{12}=L_{13}=30 \text{ mm}$ are equal to $\sigma_x = -1.269 \text{ MPa}$, and at $L_{12}=L_{13}=40 \text{ mm}$ – $\sigma_x = -1.332 \text{ MPa}$.

Fig. 3 shows stresses σ_p along the cylindrical cavity touching the right support ($p=2$) at $z=0$.

Maximum stresses σ_p occur on the left side of the cylinder (Fig. 3). This happens due to the lateral pressure of the specified load on the supports.

Maximum stresses are negative $\sigma_p = -0.3336 \text{ MPa}$ at $L_{12}=L_{13}=30 \text{ mm}$ and $\phi=2.5$ in the upper part of the cylinder. When the distance between the supports increases, the maximum stresses σ_p decrease, shifting to the horizontal axis in the direction of the load.

The graph of stresses σ_p along the cylindrical cavity touching the left support ($p=3$), is symmetrical to Fig. 3 relative to the vertical axis.

Fig. 4 shows a graph of stresses σ_ϕ along the right supporting cylindrical cavity ($p=2$) at $z=0$.

In comparison with the paper [27], where the supports are rigidly connected to the layer, the graph of stresses σ_ϕ under conditions of the contact type at the supports has the opposite sign. The maximum positive stresses occur at $L_{12}=L_{13}=30 \text{ mm}$, $\phi=2.356$ and reach $\sigma_\phi=0.08975 \text{ MPa}$. The maximum negative stresses occur at $L_{12}=L_{13}=30 \text{ mm}$, $\phi=3.927$ and reach $\sigma_\phi = -0.1094 \text{ MPa}$.

Fig. 5 shows a graph of stresses σ_z along the right supporting cylindrical cavity ($p=2$) at $z=0$.

Graph of stress σ_z has the same form as in paper [27], only the values are smaller in proportion to the angle. Maximum stress values: at $L_{12}=L_{13}=30 \text{ mm}$ and $\phi=2.5$ positive $\sigma_z = -0.068 \text{ MPa}$, at $L_{12}=L_{13}=30 \text{ mm}$ and $\phi=3,927$ negative $\sigma_z = 0.0785 \text{ MPa}$.

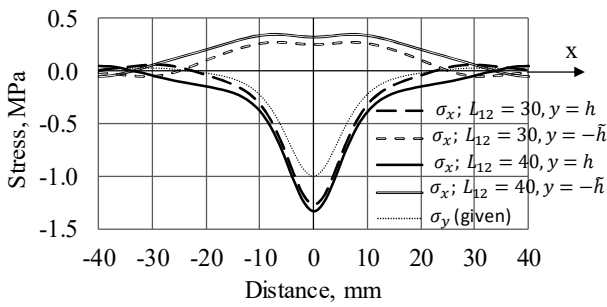


Fig. 2. Stresses on the upper and lower surfaces of the layer

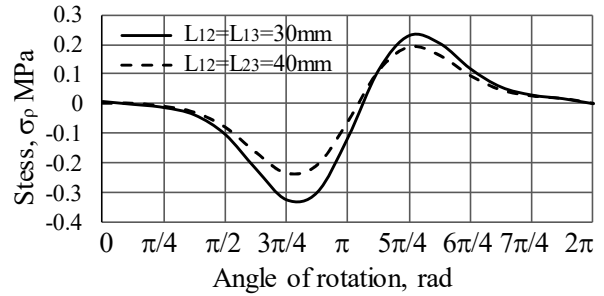


Fig. 3. Stresses σ_ρ on the surface of the cavity $p=2$

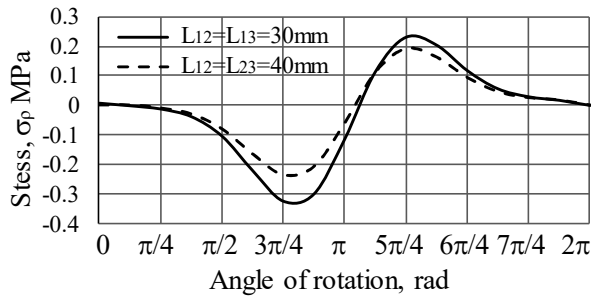


Fig. 4. Stresses σ_ϕ on the surface of the cavity $p=2$

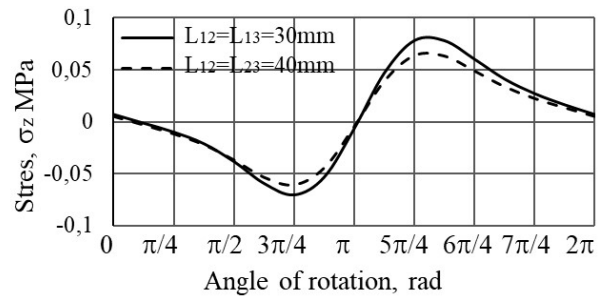


Fig. 5. Stresses σ_z on the surface of the cavity $p=2$

Fig. 6 shows a graph of stresses σ_ϕ along the cylindrical cavity $p=1$ at $z=0$.

Stresses σ_ϕ on the surface of the free cavity have mainly negative values (Fig. 6) due to the compression of this cavity between the supports by the load. Breaking (positive) stresses σ_ϕ occur only in small areas in the upper and lower part of the cavity.

When the distance between the supports increases, the maximum stresses decrease slightly (Fig. 6). Thus, the maximum stress values in the free cavity reach at $L_{12}=L_{13}=30$ mm: positive $\sigma_\phi=0.32476$ MPa, negative $\sigma_\phi=-0.7715$ MPa.

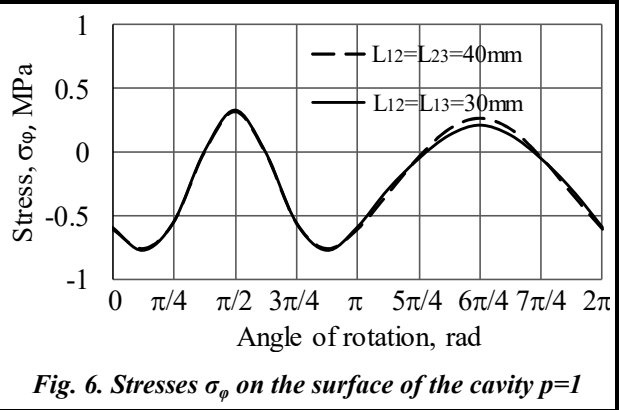


Fig. 6. Stresses σ_ϕ on the surface of the cavity $p=1$

Conclusions

A new problem has been solved for a layer located on two cylindrical swivel joints embedded into it and having one additional cylindrical longitudinal cavity.

Swivel joints are represented as longitudinal cylindrical cavities with contact type conditions (normal displacements and tangential stresses) set for them. This made it possible to reduce the problem to the classical model of the spatial theory of elasticity. To solve the problem, the analytical-numerical generalized Fourier method was applied, which allowed to obtain a solution with the specified accuracy.

A numerical analysis of the stress state was carried out. The analysis shows the distribution of normal stresses depending on the distance between the supports. The obtained results indicate that as this distance increases, the maximum stresses on the surface of the cylindrical cavity and the support surfaces decrease. At the same time, the stresses on the upper and lower surfaces of the layer increase.

The proposed solution method can be applied to a larger number of cylindrical cavities or cylindrical joints. The resulting stress state makes it possible to estimate the geometric parameters for the models designed in practice.

Further research on the topic should be conducted in the direction of adding protective layers and thick-walled cylinders.

References

1. Tekkaya, A. E. & Soyarslan, C. (2014). Finite Element Method. In: Laperrière, L. & Reinhart, G. (eds) *CIRP Encyclopedia of Production Engineering*. Berlin, Heidelberg: Springer, pp. 508–514. https://doi.org/10.1007/978-3-642-20617-7_16699.
2. Karvatskyi, A. Ya. (2018). *Metod skinchennykh elementiv u zadachakh mekhaniky sutsilnykh seredovyshch* [Finite element method in problems of continuum mechanics]: Laboratory workshop on the academic discipline: textbook. Kyiv: National Technical University of Ukraine "Igor Sikorsky Kyiv Polytechnic Institute", 391 p. (in Ukrainian).
3. Zasovenko, A. V. & Fasoliak, A. V. (2023). *Matematychni modeliuvannia dynamiky pruzhnoho pivprostoru z tsylindrychnoiu porozhnynoi, yaka pidkriplena obolonkoiu, pry osesymetrychnykh navantazhenniakh* [Mathematical modeling of the dynamics of an elastic half-medium with a cylindrical cavity reinforced by a shell under axisymmetric loads]. *Novi materialy i tekhnologii v metalurhii ta mashynobuduvanni – New materials and technologies in metallurgy and mechanical engineering*, no. 2, pp. 67–73. <https://doi.org/10.15588/1607-6885-2023-2-10> (in Ukrainian).
4. Azarov, A. D., Zhuravlev, G. A., & Piskunov, A. S. (2015). *Sravnitelnyy analiz analiticheskogo i chislennogo metodov resheniya ploskoy zadachi o kontakte uprugikh tsilindrov* [Comparative analysis of analytical and numerical methods for solving the plane problem of contact of elastic cylinders]. *Innovatsionnaya nauka – Innovative Science*, no. 1–2, pp. 5–13 (in Russian).
5. Guz, A. N., Kubenko, V. D., & Cherevko, M. A. (1978). *Difraktsiya uprugikh voln* [Elastic wave diffraction]. Kyiv: Naukova dumka, 307 p. (in Russian).
6. Grinchenko, V. T. & Meleshko, V. V. (1981). *Garmonicheskiye kolebaniya i volny v uprugikh telakh* [Harmonic vibrations and waves in elastic bodies]. Kyiv: Naukova dumka, 284 p. (in Russian).
7. Fesenko, A. & Vaysfel'd, N. (2019). The wave field of a layer with a cylindrical cavity. In: Gdoutos, E. (eds) *Proceedings of the Second International Conference on Theoretical, Applied and Experimental Mechanics. ICTAEM 2019. Structural Integrity*, vol. 8. Cham: Springer, pp. 277–282. https://doi.org/10.1007/978-3-030-21894-2_51.
8. Fesenko, A. & Vaysfel'd, N. (2021). The dynamical problem for the infinite elastic layer with a cylindrical cavity. *Procedia Structural Integrity*, vol. 33, pp. 509–527. <https://doi.org/10.1016/j.prostr.2021.10.058>.
9. Jafari, M., Chaleshtari, M. H. B., Khoramishad, H., & Altenbach H. (2022). Minimization of thermal stress in perforated composite plate using metaheuristic algorithms WOA, SCA and GA. *Composite Structures*, vol. 304, part 2, article 116403. <https://doi.org/10.1016/j.compstruct.2022.116403>.
10. Malits, P. (2021). Torsion of an elastic half-space with a cylindrical cavity by a punch. *European Journal of Mechanics – A/Solids*, vol. 89, article 104308. <https://doi.org/10.1016/j.euromechsol.2021.104308>.
11. Khechai, A., Belarbi, M.-O., Bouaziz, A., & Rekbi, F. M. L. (2023). A general analytical solution of stresses around circular holes in functionally graded plates under various in-plane loading conditions. *Acta Mechanica*, vol. 234, pp. 671–691. <https://doi.org/10.1007/s00707-022-03413-1>.
12. Smetankina, N., Kurenkov, S., & Barakhov, K. (2023). Dynamic stresses in the adhesive joint. The Goland-Reissner model. In: Cioboată D. D. (eds) *International Conference on Reliable Systems Engineering (ICoRSE) – 2023. ICoRSE 2023. Lecture Notes in Networks and Systems*. Cham: Springer, vol. 762, pp. 456–468. https://doi.org/10.1007/978-3-031-40628-7_38.
13. Ugrimov, S., Smetankina, N., Kravchenko, O., Yareshchenko, V., & Kruszka, L. (2023). A study of the dynamic response of materials and multilayer structures to shock loads. In: Altenbach H., et al. *Advances in Mechanical and Power Engineering. CAMPE 2021. Lecture Notes in Mechanical Engineering*. Cham: Springer, pp. 304–313. https://doi.org/10.1007/978-3-031-18487-1_31.
14. Smetankina, N., Merkulova, A., Merkulov, D., Misura, S., & Misiura, Ie. (2023). Modelling thermal stresses in laminated aircraft elements of a complex form with account of heat sources. In: Cioboată D. D. (eds) *International Conference on Reliable Systems Engineering (ICoRSE) – 2022. ICoRSE 2022. Lecture Notes in Networks and Systems*. Cham: Springer, vol. 534, pp. 233–246. https://doi.org/10.1007/978-3-031-15944-2_22.
15. Smetankina, N., Kravchenko, I., Merkulov, V., Ivchenko, D., & Malykhina, A. (2020). Modelling of bird strike on an aircraft glazing. In book: Nechyporuk M., Pavlikov V., Kritskiy D. (eds) *Integrated Computer Technologies in Mechanical Engineering. Advances in Intelligent Systems and Computing*. Cham: Springer, vol. 1113, pp. 289–297. https://doi.org/10.1007/978-3-030-37618-5_25.
16. Nikolayev, A. G. & Protsenko, V. S. (2011). *Obobshchennyy metod Furye v prostranstvennykh zadachakh teorii uprugosti* [Generalized Fourier method in spatial problems of the theory of elasticity]. Kharkiv: National Aerospace University "Kharkiv Aviation Institute", 344 p. (in Russian).
17. Nikolaev, A. G. & Tanchik, E. A. (2015). The first boundary-value problem of the elasticity theory for a cylinder with N cylindrical cavities. *Numerical Analysis and Applications*, vol. 8, pp. 148–158. <https://doi.org/10.1134/S1995423915020068>.

18. Nikolaev, A. G. & Tanchik, E. A. (2016). Stresses in an elastic cylinder with cylindrical cavities forming a hexagonal structure. *Journal of Applied Mechanics and Technical Physics*, vol. 57, pp. 1141–1149. <https://doi.org/10.1134/S0021894416060237>.
19. Nikolaev, A. G. & Tanchik, E. A. (2016). Model of the stress state of a unidirectional composite with cylindrical fibers forming a tetragonal structure. *Mechanics of Composite Materials*, vol. 52, pp. 177–188. <https://doi.org/10.1007/s11029-016-9571-6>.
20. Nikolayev, A. G. & Orlov, Ye. M. (2012). *Resheniye pervoy osesimmetrichnoy termouprugoy kravevoy zadachi dlya transversalno-izotropnogo poluprostranstva so sferoidalnoy polostyu* [Solution of the first axisymmetric thermoelastic boundary value problem for a transversally isotropic half-space with a spheroidal cavity]. *Problemy vychislitelnoy mekhaniki i prochnosti konstruksiy – Problems of Computational Mechanics and Strength of Structures*, iss. 20, pp. 253–259 (in Russian).
21. Ukrainets, N., Murahovska, O., & Prokhorova, O. (2021). Solving a one mixed problem in elasticity theory for half-space with a cylindrical cavity by the generalized Fourier method. *Eastern-European Journal of Enterprise Technologies*, vol. 2, no. 7 (110), pp. 48–57. <https://doi.org/10.15587/1729-4061.2021.229428>.
22. Miroshnikov, V. Yu. (2020). Stress state of an elastic layer with a cylindrical cavity on a rigid foundation. *International Applied Mechanics*, vol. 56, iss. 3, pp. 372–381. <https://doi.org/10.1007/s10778-020-01021-x>.
23. Miroshnikov, V. (2023). Rotation of the layer with the cylindrical pipe around the rigid cylinder. In: Altenbach H., et al. *Advances in Mechanical and Power Engineering. CAMPE 2021. Lecture Notes in Mechanical Engineering*. Cham: Springer, pp. 314–322. https://doi.org/10.1007/978-3-031-18487-1_32.
24. Miroshnikov, V. Yu., Medvedeva, A. V., & Oleshkevich, S. V. (2019). Determination of the stress state of the layer with a cylindrical elastic inclusion. *Materials Science Forum*, vol. 968, pp. 413–420. <https://doi.org/10.4028/www.scientific.net/MSF.968.413>.
25. Miroshnikov, V. Yu. (2019). Investigation of the stress strain state of the layer with a longitudinal cylindrical thick-walled tube and the displacements given at the boundaries of the layer. *Journal of Mechanical Engineering – Problemy Mashynobuduvannia*, vol. 22, no. 2, pp. 44–52. <https://doi.org/10.15407/pmach2019.02.044>.
26. Miroshnikov, V. Yu., Savin, O. B., Hrebennikov, M. M., & Pohrebniak, O. A. (2022). Analysis of the stress state of a layer with two cylindrical elastic inclusions and mixed boundary conditions. *Journal of Mechanical Engineering – Problemy Mashynobuduvannia*, vol. 25, no. 2, pp. 22–29. <https://doi.org/10.15407/pmach2022.02.022>.
27. Miroshnikov, V. Yu., Savin, O. B., Hrebennikov, M. M., & Demenko, V. F. (2023). Analysis of the stress state for a layer with two incut cylindrical supports. *Journal of Mechanical Engineering – Problemy Mashynobuduvannia*, vol. 26, no. 1, pp. 15–22. <https://doi.org/10.15407/pmach2023.01.015>.
28. Miroshnikov, V., Savin, O., Sobol, V., & Nikichanov, V. (2023). Solving the problem of elasticity for a layer with N cylindrical embedded supports. *Computation*, vol. 11, article 172, 11 p. <https://doi.org/10.3390/computation11090172>.

Received 23 December 2023

Аналіз напруженого стану шару з двома циліндричними шарнірами й циліндричною порожниною

В. Ю. Мірошніков, В. П. Пелих, О. Ю. Деньщиків

Національний аерокосмічний університет ім. М. Є. Жуковського «Харківський авіаційний інститут»,
61070, Україна, м. Харків, вул. Вадима Манька, 17

На практиці часто зустрічаються з'єднання у вигляді циліндричних шарнірів. Проте точні методи для розрахунку подібних моделей відсутні. З огляду на це створення алгоритмів розв'язання таких задач є актуальним. У поданій роботі розв'язана просторова задача теорії пружності для нескінченного шару з двома циліндричними шарнірами й циліндричною порожниною, розташованими паралельно одна одній та паралельно поверхням шару. Циліндричні врізані шарніри подані у вигляді порожнин із заданими на них умовами контактного типу (нормальні переміщення й дотичні напруження). На поверхнях шару і на поверхні порожнини задані напруження. Шар розглядається у декартовій системі координат, циліндричні порожнини – у локальних циліндричних. Просторова задача теорії пружності розв'язується за допомогою узагальненого методу Фур'є, які застосовуються до рівнянь Ламе. Задовольняючи граничним умовам, створюється система нескінчених лінійних алгебраїчних рівнянь, до яких застосовується метод редукції. У числовому дослідженні точність виконання граничних умов склала 10^{-3} для значень напружень від 0 до 1 при порядку системи рівнянь (членів ряду Фур'є) $t=4$. При збільшенні порядку системи рівнянь точність розрахунків збільшується. Аналіз напруженого стану проведений при різній відстані між опорами. Отримані результати свідчать, що зі збільшенням цієї відстані напруження на опорних циліндричних поверх-

нях шару і на циліндричній поверхні порожнини зменшуються. Перерозподіл цих напружень відбувається на верхню й нижню поверхні шару, де напруження збільшуються і перевищують задані. Отримані числові результати можуть бути використані при прогнозуванні геометричних параметрів під час проектування.

Ключові слова: шар з циліндричними порожнинами, узагальнений метод Фур'є, умови контактної типу.

Література

1. Tekkaya A. E., Soyarslan C. Finite Element Method. In: Laperrière L., Reinhart G. (eds) *CIRP Encyclopedia of Production Engineering*. Berlin, Heidelberg: Springer, 2014. P. 508–514. https://doi.org/10.1007/978-3-642-20617-7_16699.
2. Карвацький А. Я. Метод скінченних елементів у задачах механіки суцільних середовищ. Лабораторний практикум з навчальної дисципліни: навч. посібник. Київ: КПІ ім. Ігоря Сікорського, 2018. 391 с.
3. Засовенко А. В., Фасоляк А. В. Математичне моделювання динаміки пружного півпростору з циліндричною порожниною, яка підкріплена оболонкою, при осесиметричних навантаженнях. *Нові матеріали і технології в металургії та машинобудуванні*. № 2. С. 67–73. <https://doi.org/10.15588/1607-6885-2023-2-10>.
4. Азаров А. Д., Журавлев Г. А., Пискунов А. С. Сравнительный анализ аналитического и численного методов решения плоской задачи о контакте упругих цилиндров. *Инновационная наука*. 2015. № 1–2. С. 5–13.
5. Гузь А. Н., Кубенко В. Д., Черевко М. А. Дифракция упругих волн. Киев: Наукова думка, 1978. 307 с.
6. Гринченко В. Т., Мелешко В. В. Гармонические колебания и волны в упругих телах. Киев: Наукова думка, 1981. 284 с.
7. Fesenko A., Vaysfel'd N. The wave field of a layer with a cylindrical cavity. In: Gdoutos, E. (eds) *Proceedings of the Second International Conference on Theoretical, Applied and Experimental Mechanics. ICTAEM 2019. Structural Integrity*. Cham: Springer, 2019. Vol. 8. P. 277–282. https://doi.org/10.1007/978-3-030-21894-2_51.
8. Fesenko A., Vaysfel'd N. The dynamical problem for the infinite elastic layer with a cylindrical cavity. *Procedia Structural Integrity*. 2021. Vol. 33. P. 509–527. <https://doi.org/10.1016/j.prostr.2021.10.058>.
9. Jafari M., Chaleshtari M. H. B., Khoramishad H., Altenbach H. Minimization of thermal stress in perforated composite plate using metaheuristic algorithms WOA, SCA and GA. *Composite Structures*. 2022. Vol. 304. Part 2. Article 116403. <https://doi.org/10.1016/j.compstruct.2022.116403>.
10. Malits P. Torsion of an elastic half-space with a cylindrical cavity by a punch. *European Journal of Mechanics – A/Solids*. 2021. Vol. 89. Article 104308. <https://doi.org/10.1016/j.euromechsol.2021.104308>.
11. Khechai A., Belarbi M.-O., Bouaziz A., Rebbi F. M. L. A general analytical solution of stresses around circular holes in functionally graded plates under various in-plane loading conditions. *Acta Mechanica*. 2023. Vol. 234. P. 671–691. <https://doi.org/10.1007/s00707-022-03413-1>.
12. Smetankina N., Kurenov S., Barakhov K. Dynamic stresses in the adhesive joint. The Goland-Reissner model. In: Cioboată D. D. (eds) *International Conference on Reliable Systems Engineering (ICoRSE) – 2023. ICoRSE 2023. Lecture Notes in Networks and Systems*. Cham: Springer, 2023. Vol. 762. P. 456–468. https://doi.org/10.1007/978-3-031-40628-7_38.
13. Ugrimov S., Smetankina N., Kravchenko O., Yareshchenko V., Kruszka L. A study of the dynamic response of materials and multilayer structures to shock loads. In: Altenbach H., et al. *Advances in Mechanical and Power Engineering. CAMPE 2021. Lecture Notes in Mechanical Engineering*. Cham: Springer, 2023. P. 304–313. https://doi.org/10.1007/978-3-031-18487-1_31.
14. Smetankina N., Merkulova A., Merkulov D., Misura S., Misiura Ie. Modelling thermal stresses in laminated aircraft elements of a complex form with account of heat sources. In: Cioboată D. D. (eds) *International Conference on Reliable Systems Engineering (ICoRSE) – 2022. ICoRSE 2022. Lecture Notes in Networks and Systems*. Cham: Springer, 2023. Vol. 534. P. 233–246. https://doi.org/10.1007/978-3-031-15944-2_22.
15. Smetankina N., Kravchenko I., Merkulov V., Ivchenko D., Malykhina A. Modelling of bird strike on an aircraft glazing. In book: Nechyporuk M., Pavlikov V., Kritskiy D. (eds) *Integrated Computer Technologies in Mechanical Engineering. Advances in Intelligent Systems and Computing*. Cham: Springer, 2020. Vol. 1113. P. 289–297. https://doi.org/10.1007/978-3-030-37618-5_25.
16. Николаев А. Г., Проценко В. С. Обобщенный метод Фурье в пространственных задачах теории упругости. Харьков: Нац. аэрокосм. ун-т им. Н. Е. Жуковского «ХАИ», 2011. 344 с.
17. Nikolaev A. G., Tanchik E. A. The first boundary-value problem of the elasticity theory for a cylinder with N cylindrical cavities. *Numerical Analysis and Applications*. 2015. Vol. 8. P. 148–158. <https://doi.org/10.1134/S1995423915020068>.
18. Nikolaev A. G., Tanchik E. A. Stresses in an elastic cylinder with cylindrical cavities forming a hexagonal structure. *Journal of Applied Mechanics and Technical Physics*. 2016. Vol. 57. P. 1141–1149. <https://doi.org/10.1134/S0021894416060237>.
19. Nikolaev A. G., Tanchik E. A. Model of the stress state of a unidirectional composite with cylindrical fibers forming a tetragonal structure. *Mechanics of Composite Materials*. 2016. Vol. 52. P. 177–188. <https://doi.org/10.1007/s1029-016-9571-6>.

20. Николаев А. Г., Орлов Е. М. Решение первой осесимметричной термоупругой краевой задачи для трансверсально-изотропного полупространства со сфероидальной полостью. *Проблемы вычислительной механики и прочности конструкций*. 2012. Вып. 20. С. 253–259.
21. Ukrayinets N., Murahovska O., Prokhorova O. Solving a one mixed problem in elasticity theory for half-space with a cylindrical cavity by the generalized Fourier method. *Eastern-European Journal of Enterprise Technologies*. 2021. Vol. 2. No. 7 (110). P. 48–57. <https://doi.org/10.15587/1729-4061.2021.229428>.
22. Miroshnikov V. Yu. Stress state of an elastic layer with a cylindrical cavity on a rigid foundation. *International Applied Mechanics*. 2020. Vol. 56. Iss. 3. P. 372–381. <https://doi.org/10.1007/s10778-020-01021-x>.
23. Miroshnikov V. Rotation of the layer with the cylindrical pipe around the rigid cylinder. In: Altenbach H., et al. *Advances in Mechanical and Power Engineering. CAMPE 2021. Lecture Notes in Mechanical Engineering*. Cham: Springer, 2023. P. 314–322. https://doi.org/10.1007/978-3-031-18487-1_32.
24. Miroshnikov V. Yu., Medvedeva A. V., Oleshkevich S. V. Determination of the stress state of the layer with a cylindrical elastic inclusion. *Materials Science Forum*. 2019. Vol. 968. P. 413–420. <https://doi.org/10.4028/www.scientific.net/MSF.968.413>.
25. Miroshnikov V. Yu. Investigation of the stress strain state of the layer with a longitudinal cylindrical thick-walled tube and the displacements given at the boundaries of the layer. *Journal of Mechanical Engineering – Problemy Mashynobuduvannia*. 2019. Vol. 22. No. 2. P. 44–52. <https://doi.org/10.15407/pmach2019.02.044>.
26. Miroshnikov V. Yu., Savin O. B., Hrebennikov M. M., Pohrebniak O. A. Analysis of the stress state of a layer with two cylindrical elastic inclusions and mixed boundary conditions. *Journal of Mechanical Engineering – Problemy Mashynobuduvannia*. 2022. Vol. 25. No. 2. P. 22–29. <https://doi.org/10.15407/pmach2022.02.022>.
27. Miroshnikov V. Yu., Savin O. B., Hrebennikov M. M., Demenko V. F. Analysis of the stress state for a layer with two incut cylindrical supports. *Journal of Mechanical Engineering – Problemy Mashynobuduvannia*. 2023. Vol. 26. No. 1. P. 15–22. <https://doi.org/10.15407/pmach2023.01.015>.
28. Miroshnikov V., Savin O., Sobol V., Nikichanov V. Solving the problem of elasticity for a layer with N cylindrical embedded supports. *Computation*. 2023. Vol. 11. Article 172. 11 p. <https://doi.org/10.3390/computation11090172>.